"*Physics of Auroral Phenomena", Proc. XXXIV Annual Seminar, Apatity, pp. 137 - 142 2011*

Polar
Geophysical
Institute

TOPSIDE IONOSPHERE He^+ DENSITY DEPLETIONS: LONGITUDINAL OCCURRENCE PROBABILITY FOR VERNAL AND WINTER SEASONS

L.N. Sidorova, S.F. Filippov *(Pushkov Institute of Terrestrial Magnetism, Ionosphere and Radiowave Propagation, IZMIRAN, 142190 Troitsk, Moscow region, Russia; E-mail: lsid@izmiran.ru)*

Abstract. The idea of an equatorial origin of the He^+ density depletions was validated once again. For this aim their longitudinal occurrence distributions (P_{He+}) were obtained for vernal equinox and winter solstice in the different hemispheres. The detailed comparative analysis with the same occurrence distributions of the equatorial F region irregularities (EFI, $P_{\sigma>0.5\%}$, $P_{\sigma>0.51\%}$, $P_{\sigma>0.3\%}$), equatorial spread F (EFS, P_{RSF}) and equatorial plasma bubbles (EPB, P_{B650}) was made. The best conformity was obtained for vernal equinox. Rather different longitudinal P_{He+} pictures were revealed in the different hemispheres during winter solstice. It was found, however, that the P_{He+} variations of the Northern Hemisphere are the most similar to P_{RSF}, $P_{\sigma>0.51\%}$ and $P_{\sigma>0.5\%}$ variations. Other part of the equatorial plots ($P_{\sigma>0.3\%}$, P_{B650}) has surprisingly good similarity with P_{He+} in the Southern Hemisphere. The obtained results may be considered as new evidence supported the idea about plasma bubble origin of the He^+ density depletions.

1. Introduction

He^+ density depletions were repeatedly observed by many investigators from the first decade of spacecraft observations. They were observed in the low- and mid-latitude regions (L=1.3-3.5, ±20°-58°Λ) of the topside ionosphere. Firstly these structures were mentioned by Taylor et. al. (1971) based on the OGO-4 data. Taylor and Cordier (1974) called them as ***subtroughs*** and identified as plasma depletions distinctly observed equatorward of the light ion troughs. Subtroughs were seen by (Ershova et al., 1977; Sivtseva et al., 1982) based on the Oreol-1,-2 data. They were detected either under disturbed conditions (or several hours after storm) in the external plasmasphere or under completely quiet geomagnetic conditions deeply inside of plasmasphere (L~1.3-3.5). Worthy note that until 1996 the subtroughs were observed in case-to-case basis only (~100 cases). The huge subtrough dataset was presented by Sidorova and Ruzhin (1996) on the ISS-b observations (RRL, 1983, 1985). Subtroughs were detected in the latitude interval from ~20° up to 58°Λ (L~1.3-3.5) during high solar activity (1978-1979, $F_{10.7}$~200) at the topside ionosphere altitudes (~1100 km). There were ~700 cases in ~4000 satellite passes. It was shown that the He^+ density subtroughs are not so unique and seldom structure as it was supposed earlier. Later the subtrough statistics in respect to season, LT and longitude was obtained by Karpachev and Sidorova (1999, 2000a, 2000b, 2003). It was pointed (Karpachev and Sidorova, 2002) that the subtroughs can be divided into two groups. One group (~256 cases) is usually detected during the magnetic disturbances (or immediately after them) within ±45-58°Λ. Another group (~400 cases) appears during the prolonged magnetically quiet periods within ±20-50°Λ. It was suggested that these groups are of different origin (Karpachev and Sidorova, 2002).

An examination of the theoretical works reveals that as usually the subtroughs were interpreted as "plasmatails" resulting from earlier storm time depletions. According to the magnetospheric convection model (Chen et al., 1975) the "plasmatails" would tend to be frozen in the outer layers of the external plasmasphere. Apparently, only one part of the subtroughs observed during storms could be interpreted in this way. As to the subtroughs, observed deeply inside the plasmasphere without any connection with disturbances, it was proposed by Sidorova (2004) to consider them of an equatorial origin. This idea was put forward after comparative analyses of He^+ density depletion (subtrough) and equatorial spread-F (ESF), plasma bubble, vertical plasma drift characteristics. It was suggested that ESF/plasma bubbles and He^+ density depletions may be considered as phenomena of the same plasma bubble origin (Sidorova, 2007). It means that plasma bubbles, reaching the topside ionosphere altitudes, are mostly seen not in Ne density but in He^+ density. Why? Plasma bubbles are not "visible" in Ne (O^+) since surrounding Ne density becomes comparable with the same bubble density. Meanwhile, the plasma bubbles become "visible" in minor species (i.e. in He^+) since the background in He^+ density strongly increases in the topside ionosphere and shows contrast with insignificant small He^+ density content inside of plasma bubble (Sidorova, 2007, 2008).

Statement of the problems. According to (Sidorova, 2007) there is a good enough correlation (R~0.67) between ESF and He^+ density depletion occurrence rates plotted as functions of a season and local time. ESF statistics were derived from ground-based ionograms obtained over Brazilian regions (Abdu et al., 2000) during similar solar activity (1980-81, $F_{10.7}$ ~230). It is reasonable to ask: why the regional map (ESF statistics) and the global map (He^+ density depletion statistics) are so good correlated? Probably, the cause is hidden in the features of the longitudinal distributions of the both phenomena. Obviously, the validation of the obtained results is possible if we have the detailed *longitudinal statistics* of the He^+ density depletions and can compare with the same statistics of other equatorial plasma irregularities.

Comparable data

It should remind that He^+ density depletions are considered as originating from equatorial middle-/large-scale plasma bubbles or as possible fossil bubble signatures (Sidorova, 2007, 2008). It was supposed that plasma bubbles, produced by collision Rayleigh-Taylor instability at the bottomside of the F-layer, could rise up to the topside ionosphere and plasmasphere altitudes and seen as He^+ density depletions. Namely, equatorial plasma and separate irregularities uplift (due to vertical plasma drift) to the topside ionosphere. Large irregularities like plasma bubbles spread (due to diffusion processes) along the magnetic tubes. Their spreading becomes more and more significant in process of their uplifting. So extended bubbles look like 'bananas' with the extremities reaching the ionosphere heights (may be) in both the hemispheres (e.g., Abdu et al., 2000). Such structures could be detected by satellites as subtroughs or depletions not only above the equator but also in the low-latitudinal region. In the other hand, ESF registered as spread of traces of F region echoes on ionograms results from small-scale (small-amplitude) equatorial ionosphere irregularities. There are indications (McClure et al., 1998) that the detection of the small-amplitude irregularities (as ESF) usually means a bubble is nearby. According to Aggson et al. (1992) a ~100 km halo of such irregularities typically surrounds each plasma bubble. These irregularities could exist not only around and within the bubbles but also along the wake that plasma bubble produces (Woodman and La Hoz, 1976). Tsunoda (1980) point that ESF observed at equatorial latitudes represent bottomside irregularities that may be or may not be associated with plasma bubbles that grow into the topside ionosphere, whereas the spread F observed in low latitude ionograms can be indicative of equatorial topside plasma bubble irregularities. (ESF observations used in this study are registered within ±20° DIPLAT). So, if we suppose that the observed He^+ density depletions are of equatorial origin, it means that the main features of the equatorial F-region irregularities should be reflected in the features of the plasma bubbles, seen as the He^+ density depletions. Hence it seems reasonable to assume that the seasonal/longitudinal (s/l) variations of the He^+ density depletion statistical plots will be similar enough to the same statistics of the typical equatorial phenomena as ESF, equatorial F region irregularities (EFI) and equatorial F region plasma bubbles (EPB). Let's verify this assumption.

He^+ density depletions. Some s/l statistical characteristics of the He^+ density depletions were obtained earlier (Karpachev and Sidorova, 2000b; Sidorova, 2004). ISS-b spacecraft (35° orbital inclination) observations were used (RRL, 1983-85). The available statistics has been revised and added. The data taken within ±20-50° INVLAT and gathered in each geomagnetic longitudinal interval of 15° were considered for Northern and Southern Hemispheres separately. Each season has been presented by four-month intervals, which were centered around a solstice/equinox accordingly. For example, spring season was considered for the period of two months before and after spring equinox day (March 22), i.e. from January 22 to May 22. Evidently, such season fractioning implies partial data overlapping. However this approach has been caused by peculiarities of the available dataset: there were many gaps in the ISS-b measurement dataset. Note that the He^+ density subtroughs with density depletions from two times to two orders of magnitude of the background plasma density (Karpachev and Sidorova, 2002) were taken into account. The obtained P_{He+} histograms with spline smoothing curves (factor 2.2) are presented in Fig. 1(top and bottom).

Equatorial F region irregularities (EFI). EFI statistics was taken from the different satellite observations (Tables 1). The most valuable patterns were taken from (McClure et al., 1998), where all results were presented in very convenient form. (It was favorable case to find this study!). Note that the most of these plots have been obtained for 1978-80 or for the years of the same solar activity. The brief data characteristics are shown below.

a) S/l occurrence patterns were derived by McClure et al. (1998) from ion number density (N_i) data from ion drift meter on AE-E (19.76° orbital incl.). N_i data from 19 to 06 LT and within ±20° DIPLAT, where most bubbles are found, were under consideration. Only values with σ>0.5% were taken into account. (σ is normalized irregularity index; $\sigma=\Delta N_i/\overline{N_i}$, where $\overline{N_i}$ is the average of ion density, ΔN_i is a standard deviation of the background density.) The device characteristics and used experimental technique allowed to detect the irregularities space-sized from 50 to 1000 km. EFI statistics ($P_{\sigma>0.5\%}$) has been calculated as average for three-month intervals. (These intervals entirely coincide with the intervals used in present work.) S/l variations of EFI statistics are shown in Fig. 1by thin black curves.

b) S/l variations of EFI statistics were obtained by Su et al. (2006) on the base of N_i data from ROCSAT (circular orbit, 35° orbital incl.). Calculations were made within l ±15° DIPLAT for one month of each season (e.g., December, March). The statistical occurrence distribution of EFI has been studied for many years (1999-2004). The data were obtained during high (1999-2003, $F_{10.7}$=140÷190, 23^{-rd} cycle) and moderate (2003-2004, $F_{10.7}$=110÷130) solar activity. High solar activity period was dominated that is why it was possible to use the obtained EFI statistical results for comparison. Ion irregularity values with σ>0.3% were taken into account. Due to high spatial resolution it was possible to detect the ion irregularities in characteristic scale length between 7.5 km to 75 km. However $P_{\sigma>0.3\%}$ for the ROCSAT observation is noted to be about half of that derived from (e. g.) the AE-E data (McClure, 1998) because of different selection criteria. The s/l variations of the EFI statistics are shown in Fig. 1 by dotted curves. The scale of the plots is on the right.

Table 1. Comparable studies, data sources, geophysical parameters and space/time coverage.

Study	**Data**	**Parameter**	**LT interval**	**Altitudes**	**Latitudes**	**Years**	**$F_{10.7}$**
Present study	ISS-b	P_{He+}	20-04 LT	~1100 km	±20÷50° INVLAT	1978-80	150÷220
Maryama and Matuura, 1980	ISS-b	P_{RSF}	18-06 LT	~1100 km	±20° DIPLAT	1978-80	150÷220
McClure et al., 1998	AE-E	$P_{\sigma>0.5\%}$	19-06 LT	300-475 km	±20° DIPLAT	1978-80	150÷220
Watanabe, Oya, 1986	Hinotori	P_{B650}	19-06 LT	650 km	±20° DIPLAT	1981	~200
Basu et al., 1976	OGO-6	$P_{\sigma>0.51\%}$	18-06 LT	400-500 km	±20° DIPLAT	1969-70	~150
Su et al., 2006	ROCSAT	$P_{\sigma>0.3\%}$	18-06 LT	~600 km	±15° DIPLAT	1999-04	110÷190
Study	**Data**	**Parameter**	**LT interval**	**Altitudes**	**Latitudes**	**Years**	**$F_{10.7}$**

c) The results derived by Basu et al. (1976) from N_i data from the OGO-6 spacecraft (90° orbital incl.) were also used for comparison. Longitudinal variations of EFI statistics were calculated for one winter season (November-December, 1969-70) in the interval ±20 DIPLAT. Only ion irregularities with σ>0.51% from 400÷500 km altitudes were taken into account. EFI statistics ($P_{\sigma>0.51\%}$) are shown in Fig. 1 by thick dark grey curve.

Equatorial spread F. As it is well known the small irregularities (1÷10 км) or so called “noise” are simply detected as equatorial spread-F (ESF). ESF statistics as function of longitude was found by Maryama and Matuura (1980). The authors have used the data from ISS-b spacecraft. They have used RSF parameter defined as range-spreading parameter: an occurrence probability P_{RSF} of one and more range gates darkened on single ionogram by topside bubbles and irregularities. P_{RSF} values, obtained in the interval of ±20 DIPLAT, have been divided into three 4-month seasonal intervals. Unfortunately, these intervals have not been centered around a solstice/equinox, i.e. there is ~80% overlapping intervals used before. S/l variations of the RSF statistics (P_{RSF}) are shown in Fig.1 by thin grey curves.

Equatorial plasma bubbles of F region (EPB). Since the present work is devoted to the problem of plasma bubble evolution at the topside ionosphere heights, it is extremely desirable to have an information about the equatorial plasma bubbles (EPB) in F region. These information has been found in (Watanabe and Oya, 1986) based on N_i measurement data obtained from Hinotori spacecraft (31° orbital inclination) during high solar activity year (1981, $F_{10.7}$~200). Longitudinal EPB statistics were calculated in the interval ±20 DIPLAT. Each season is presented as average for three-month interval. Seasonal intervals fall within our 4-moths intervals and approximately centered around a solstice/equinox. S/l variations of the EPB probability (P_{B650}) are shown in Fig. 1 by thick light grey curve.

3 The comparative analysis

It is necessary to note that all results used for comparison were received under the same solar and geophysical conditions (local time, season, solar activity level). F region observations were made during the same LT interval 18(19)-06 LT. However LT interval of the He^+ density depletion observations has been intentionally chosen more narrow (20-04 LT). To our mind, this choice is more adequate for sunset-night time at the topside ionosphere heights (~1100 km). The longitudinal occurrence rates for two different seasons (winter and vernal) were under consideration. Firstly, let’s focus on the equinox period, when there are approximately equal conditions for the different hemispheres.

Vernal conditions. As it was expected, studied the P_{He+} variations appear to be the most similar to the P_{RSF} variations (Maryama and Matuura, 1980), derived from ISS-b data (Fig.1). Really, if the hypothesis about an equatorial origin of He^+ density depletions is true, the results received from the data of one satellite should be similar as much as possible. In other words, an equatorial picture (±20° DIPLAT) of the longitudinal occurrence probability (P_{RSF}) should be as much as possible similarly projected in the latitudinal intervals ±20÷50° INVLAT of the different hemispheres. (Certainly, it is fair if we bear in mind the magnetic field differences in the different hemispheres.) And really, this assumption is validated (Fig.1). So, the P_{He+} variations of the both hemispheres are similar to the equatorial statistical plots. Moreover, note that the P_{He+} peaks appear approximately at the same longitudes as P_{RSF}. Comparison with $P_{\sigma>0.5\%}$ (McClure et al., 1998) and $P_{\sigma>0.3\%}$. (Su et al., 2006) also reveals good similarity in the shape of the longitudinal variations. The similarity becomes the most convincing if we examine minor and “thin” details of the plots. So, according to the EFI data the local maxima (longitudes ~180° and ~270°) are well visible. Moreover, they are distinctly pronounced in the P_{He+} plots.

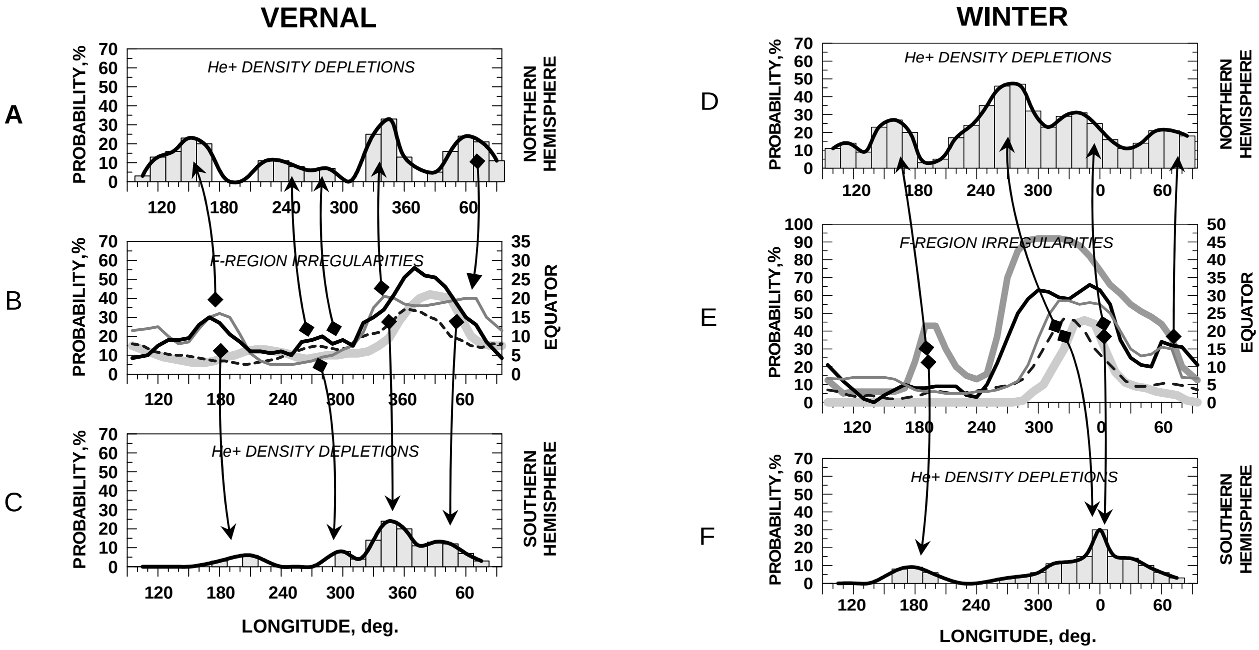

Let's consider another fact. It is easy to notice that bifurcation of the main EFI probability maximum only slightly pronounced in statistics of Su et al. (2006) is clearly visible in the statistics of McClure et al. (1998).

Fig. 1. Longitudinal distributions of P_{He+} (histograms and smoothing curves) calculated for VERNAL and WINTER from the ISS-b data within ±20-50° INVLAT in the Northern (a, d) and Southern (c, f) Hemispheres. Longitudinal distributions of $P_{\sigma>0.5\%}$, $P_{\sigma>0.3\%}$, P_{RSF}, P_{B650} obtained within the equatorial region (±20° DIPLAT) (b, e). $P_{\sigma>0.5\%}$ (McClure et al., 1998) is shown by thin black line. P_{B650} (Watanabe and Oya, 1986) is shown by thick light grey line. P_{RSF} (Maryama, Matuura, 1980) is shown by thin grey line. $P_{\sigma>0.3\%}$ (Su et al., 2006) (dotted line) is presented by right scale. $P_{\sigma>0.51\%}$ (Basu et al., 1976) is shown for WINTER (e) by thick dark grey line.

According to Maryama and Matuura (1980) the bifurcated maximum is already very well pronounced structure which is distinctly reflected in the P_{He+} plots of the both hemispheres. Comparison with the longitudinal statistics of the plasma bubbles (P_{B650}) shows no so good similarity. Nevertheless, the main tendency takes place as before.

According to the theory the major cause for the longitudinal irregularity occurrence is an alignment of the sunset terminator with the magnetic meridian (Abdu et al., 1981; Tsunoda, 1985). Maximum uplift of irregularities is expected in so called "node seasons" (equinox seasons), when the sunset terminator and magnetic meridian are nearly parallel. It seems this conclusion is also fair for He^+ density depletion occurrence, if we suppose that EFIs and He^+ density depletions are of the same equatorial origin. That is why the P_{He+} plots of the different hemispheres are of almost the same intensity and practically equally developed. What about some discrepancy in the shape of the P_{He+} curves in the different hemispheres? Apparently, it can be explained by superposition of some factors. First of all, the light differences in the shape of variations are caused by features of the magnetic field of the different hemispheres or so-called "magnetic declination effect".

Winter conditions. The most dramatic insolation differences take place for the different hemispheres during winter solctice. Apparently, it should expect the significant differences of P_{He+} in the different hemispheres. Let's consider the plot in the Northern Hemisphere (NH). It is easy to notice good enough similarity between the P_{He+} curve and the most part of the equatorial plots. It is possible to see the clear tendency of the distortion of the main maximum of the equatorial plots, which finally "develops" in the P_{He+} plot. So, the main maximum appeared as widened peak in $P_{\sigma>0.51\%}$ (Basu et al., 1976) is seen with slightly outlined bifurcation in P_{RSF} (Maryama and Matuura, 1980) and with twin peaks in $P_{\sigma>0.5\%}$ (McClure et al., 1998). At last this bifurcated maximum turn into the P_{He+} maximum with two separate crests and deep internal valley. The main $P_{\sigma>0.51\%}$ maximum covers the longitudes of 240°-30°. The main bifurcated P_{He+} maximum appears almost at the same longitudes however with light shifting in respect to other main equatorial peaks. Worthy note that the "thin" details of the EFI statistical plots are also "developed" in the P_{He+} curve. The minor local $P_{\sigma>0.5\%}$ and P_{RSF} maxima near 60° longitude also appear in the NH as minor local maximum of P_{He+}. Local P_{He+} maximum near 150°÷180° longitude needs in special comments. It is possible to doubt about a reliability of this second P_{He+} peak. However, any doubt disappears when we see the similar second maximum in the $P_{\sigma>0.51\%}$ pattern (Basu et al., 1976) and the small but clear amplitude growth of $P_{\sigma>0.5\%}$ (McClure et al., 1998).

Another part of the equatorial plots ($P_{\sigma>0.3\%}$ (Su et al., 2006), P_{B650} (Watanabe and Oya, 1986)) has surprisingly good similarity with the P_{He+} curve in the Southern Hemisphere (SH) (Fig. 1). The main maxima of the $P_{\sigma>0.3\%}$,

P_{B650} statistics are more narrow and less intensive; their tops are of simple form like the P_{He+} curve in the SH. Moreover, the main maximum of P_{B650} near 360° longitude appears in P_{He+} at the same longitudes. And again the local $P_{\sigma>0.51\%}$ maximum (Basu et al., 1976) near 180° longitude is still clearly visible in P_{He+} curve of the SH.

Thus we should conclude that there are the most significant differences in the P_{He+} distributions of the different hemispheres for solstice periods. The P_{He+} variations in one hemisphere are strongly deformed in comparison with the P_{He+} variations of other hemisphere. Moreover some P_{He+} peaks appear with longitudinal shifts. However, even so different P_{He+} pictures have the common features with the equatorial irregularity occurrence distributions. Note that the comparison was done not for one dataset but for several datasets (EFI, ESF, EPB) obtained by the different investigators on the base of the different observations. It seems this fact is the most valuable one for this study. Availability of the sufficient statistics supplies not only reliability but also the "repeatable" results. Moreover, this fact allows to see a tendency in the EFI dynamics subsequently developed in the P_{He+} curves of the SH and NH. We should conclude once again that all data involved in comparison show that the main geophysical characteristics of the equatorial F region irregularities really repeat in new results. The obtained results have all main features repeated even in the details.

Apparently, the seasonal factor should be considered as a factor of the first approximation. Due to seasonal factor only the more favorable conditions for plasma bubble "survival" can appear in one hemisphere and, on the contrary, less favorable conditions can appear in other hemisphere. The thermosphere meridional winds, depending on a season, play the important role in these processes. They can suppress the irregularity development in F region during irregularity generation due to inhibiting the growth of Reyleigh-Taylor instability and flux tube integrated conductivity (e. g., Abdu, 2001). As result they can "lock" the plasma bubble development in one hemisphere and, on the contrary, favor them in another hemisphere (e.g., Abdu, 2001; Sidorova, 2008). The magnetic declination effect also makes significant amendments to the processes above equator and low latitudes. In particular, there are indications that the magnetic declination effect control the seasonal occurrence probability of EFI and ESF (Tsunoda, 1985; Abdu et al., 1992). In other words, the occurrence probability of EFI and ESF essentially increases, when there is a small angle between the sunset terminator and magnetic meridian. It seems the combination of two main factors (seasonal peculiarities and the magnetic declination effect) generates the preference/suppression mode, which "works" for ***some longitudes*** in one hemisphere and for ***other longitudes*** in other hemisphere. As a result, the plasma bubble occurrence distribution can be minimally deformed and shifted in one hemisphere in relation to primary equatorial picture and more strongly deformed (or absolutely "suppressed") in other hemisphere under the "bad" conditions.

2. Conclusions

The longitudinal occurrence distributions of the He^+ density depletions were obtained for vernal and winter seasons in the different hemispheres. The obtained characteristics were compared with the longitudinal occurrence distributions of the equatorial F region irregularities (EFI), equatorial spread F (EFS) and equatorial plasma bubbles (EPB).

1. It was found for ***vernal equinox*** that: (a) The P_{He+} plots of the different hemispheres are of almost the same intensity and practically equally developed. The light shape difference of the P_{He+} plots of the different hemispheres can be explained by superposition of some factors. First of all, it is caused by magnetic declination effect. (b) The main longitudinal occurrence probability maxima of the equatorial F region irregularities (EFI, ESF, EPB) are well enough reflected in the P_{He+} plots of the both hemispheres.

2. It was found for ***winter solstice*** that: (a) Rather different longitudinal P_{He+} pictures appear in the different hemispheres. It was suggested that at least two major factors are responsible for discrepancy of the P_{He+} plots. The deviations are caused by seasonal peculiarities of the different hemispheres (insolation and meridional winds) and by magnetic declination effect. (b) The P_{He+} variations have the common features with the equatorial irregularity occurrence distributions. P_{RSF} (Maryama and Matuura, 1980), $P_{\sigma>0.51\%}$ (Basu et al., 1976) and $P_{\sigma>0.5\%}$ (McClure et al., 1998) are the most similar to the P_{He+} plot in the Northern Hemisphere. Other part of the equatorial plots ($P_{\sigma>0.3\%}$ (Su et al., 2006), P_{B650} (Watanabe, Oya, 1986)) has surprisingly good similarity with the P_{He+} plot in the Southern Hemisphere.

3. All mentioned results obtained in this study may be considered as new evidence supported the idea about the plasma bubble origin of the He^+ density depletions.

Acknowledgements. We express our gratitude to ISS Research and Operation Committee (Japan) for providing the ISS-b data, M.A. Abdu (Brazil), T. Maruyama (Japan) for the useful advices and discussions. This work was partly supported by Russian Foundation for Basic Research (RFBR) under grant № 09-05-01071-a.

References

Abdu, M.A., Bittencourt, J.A., Batista, I.S., 1981. Magnetic declination control of the equatorial F region dynamo electric field development and spread F. J. Geophys. Res. 86(A103), 11443-11446.

Abdu, M.A., Batista, I.S., Sobral, J.H.A., 1992. A new aspect of magnetic declination control of the equatorial spread F and F region dynamo. J. Geophys. Res. 97(A10), 14897-14904.

Abdu, M.A., Sobral, J.H.A., Batista, I.S., 2000. Equatorial spread F statistics in the american longitudes: some problems relevant to ESF description in the IRI scheme. Adv. Space Res. 25, 113-124.

Abdu, M.A., 2001. Outstanding problems in the equatorial ionosphere-thermosphere electrodynamics relevant to spread F. J. Atmos. Terr. Phys. 63, 869-884.

Aggson, T.L., Maynard, N.C., Hanson, W.B., Saba, J.L., 1992. Electric field observations of equatorial bubbles. J. Geophys. Res. 97(A3), 2997-3009.

Basu, Su., Basu, S., Khan, B.K., 1976. Model of equatorial scintillation from in-situ measurements. Radio. Sci. 11, 821-832.

Chen, A.J., Grebowsky, J.M., Taylor, H.A., 1975. Dynamics of mid-latitude light ion trough and plasma tails. J. Geophys. Res. 80(7), 968-976.

Erschova, V.A., Sivtseva, L.D., Cranie, J., Blan, E., Sovo, J.-A., 1977. Geophysical results of mass-spectrometer measurements (in Russian). Space Research, 15(2), 277-285.

Karpachev, A.T., Sidorova, L.N., 1999. Detection of the trough and subtrough in the light ion density from ISS-b satellite data at altitudes of ~1100 km. Geomagn. Aeron. 39(3), 318-325.

Karpachev, A.T., Sidorova, L.N., 2000a. Probability of occurrence the midlatitude trough and low-latitude subtrough in He^+ density as a function of season, local time, and magnetic activity. Geomagn. Aeron. 40(2), 156-165.

Karpachev, A.T., Sidorova, L.N., 2000b. Longitudinal variations in the probability of observation of the trough and subtrough in He^+ ion density under nighttime conditions. Geomagn. Aeron. 40(5), 592-602.

Karpachev, A.T., Sidorova, L.N., 2002. Occurrence probability of the light ion trough and subtrough in He^+ density on season and local time. Adv. Space Res. 29(6), 999-1008.

Karpachev, A.T., Sidorova, L.N., 2003. Distinction and classification of the troughs and subtroughs in He^+ density from ISS-b satellite data at 1000-1200 km altitudes. J. Atm. Solar-Terr. Phys. 65, 997-1006.

Maryama, T., Matuura, N., 1980. Global distribution of occurrence probability of spread echoes based on ISS-b observation. J. Radio Res. Lab. 27(124), 201-216.

McClure, J.P., Singh, S., Bamgboye, D.K., Johnson, F.S., Kil, H., 1998. Occurrence of equatorial F region irregularities: Evidence for tropospheric seeding. J. Geophys. Res. 103(A12), 29119-29135.

RRL, 1983. Summary Plots of Ionospheric Parameters obtained from Ionosphere Sounding Satellite-b. Tokyo: Radio Research Laboratories Ministry of Posts and Telecommunications. 1-3.

RRL, 1985. Summary Plots of Ionospheric Parameters obtained from Ionosphere Sounding Satellite-b. Tokyo: Radio Research Laboratories Ministry of Posts and Telecommunications. Special Report. 4.

Sidorova, L.N., Ruzhin, Yu.Ya., 1996. Peculiarities of the low-latitudinal trough in He^+ during high solar activity period, in: Proceedings of 31st Scientific Assembly of COSPAR. University of Birmingham, England, p. 91.

Sidorova, L.N., 2004. He^+ density topside modeling based on ISS-b satellite data. Adv. Space Res. 33(6), 850-854.

Sidorova, L.N., 2007. Plasma bubble phenomenon in the topside ionosphere. Adv. Space Res., Special issue (COSPAR). 39, 1284-1291, doi: 10.1016/j.asr.2007.03.067.

Sidorova, L.N., 2008. Topside plasma bubbles, seen as He^+ density depletions, in: Proceedings of Conference on Fundamental Space Research. Sunny Beach, Bulgaria, pp. 238-241.

Sivtseva, L.D., Erschova, V.A., Mosova, Z.A., 1982. Low-latitude H^+ density trough in upper ionosphere (in Russian), in: Schafer, G.V. (Ed.), Bulletin of Scientific Technical Information, Space Physics and Aeronomy Problems. Proceedings of Yakutsk Department, SO AN USSR, Yakutsk, pp. 39-40.

Su, S.-Y., Liu, C.H., Ho, H.H., Chao, C.K., 2006. Distribution characteristics of topside ionospheric density irregularities: Equatorial versus midlatitude regions. J. Geophys. Res. 111, A06305, doi: 10.1029/2005JA011330.

Taylor, H.A., Jr., Grebowsky, J.M., Walsh, W.J., 1971. Structured variations of the plasmapause: Evidence of a corotating plasma tail. J. Geophys. Res. 76(28), 6806-6814.

Taylor, H.A., Cordier, G.R., 1974. In situ observations of irregular ionospheric structure associated with the plasmapause. Planet. Space Sci. 22(9), 1289-1296.

Tsunoda, R.T., 1980. Magnetic field aligned characteristics of plasma bubbles in the nighttime equatorial ionosphere. J. Atmos. Terr. Phys. 42, 743-752.

Tsunoda, R.T., 1985. Control of the seasonal and longitudinal occurrence of equatorial scintillations by the longitudinal gradient in untegrated E region Pedersen conductivity. J. Geophys. Res. 90, 447-456.

Watanabe, S., Oya, H., 1986. Occurrence characteristics of low latitude ionospheric irregularities observed by impedance probe on board the Hinotori satellite. J. Geomagn. Geoelectr. 38, 125-149.

Woodman, R.F., La Hoz, C., 1976. Radar observations of F-region equatorial irregularities. J. Geophys. Res. 81(31), 5447-5466, doi:10.1029/JA081i031p05447.